JOURNAL OF GEOPHYSICAL RESEARCH, VOL. 108, NO. B11, 2512, doi:10.1029/2002JB002098, 2003

Rheology and strength of the Eurasian continental lithosphere in the foreland of the Taiwan collision belt: Constraints from seismicity, flexure, and structural styles

Frédéric Mouthereau and Carole Petit
Laboratoire de Tectonique, Université P and M Curie, Paris, France

Received 16 July 2002; revised 23 June 2003; accepted 14 July 2003; published 5 November 2003.

[1] Deformation in western Taiwan is characterized by variable depth-frequency distribution of crustal earthquakes which are closely connected with along-strike variations of tectonic styles (thin or thick skinned) around the Peikang High, a major inherited feature of the Chinese margin. To fit the calculated high crustal geotherm and the observed distribution of the crustal seismic activity, a Qz-diorite and granulite composition for the upper and the lower crust is proposed. We then model the plate flexure, through T_e estimates, using brittle-elastic-ductile plate rheology. Flexure modeling shows that the best fit combination of T_e-boundary condition is for thrust loads acting at the belt front. The calculated T_e vary in the range of $\sim$15–20 km. These values are primarily a reflection of the thermal state of the rifted Chinese margin inherited from the Oligocene spreading in the South China Sea. However, other mechanical properties such as the degree of crust/mantle coupling and the thickness of the mechanically competent crust and mantle are considered. South of the Peikang High, flexure modeling reveals lower T_e associated with thinner mechanically strong layers. Variable stress/strain distribution associated with a higher degree of crust/mantle decoupling is examined to explain plate weakening. We first show that plate curvature cannot easily explain strength reduction and observed seismic activity. Additional plate-boundary forces arising from the strong coupling induced by more frontal subduction of a buoyant crustal asperity, i.e., the Peikang High, with the overriding plate are required. Favorably oriented inherited features in the adjacent Tainan basin produce acceleration of strain rates in the upper crust and hence facilitate the crust/mantle decoupling as attested by high seismic activity and thick-skinned deformation. The relative weakening of the lower crust and mantle then leads to weaken the lithosphere. By contrast, to the north, more oblique collision and the lack of inherited features keep the lithosphere stronger. This study suggests that when the Eurasian plate enters the Taiwan collision, tectonic inheritance of the continental margin exerts a strong control on the plate deformation by modifying its strength. *INDEX TERMS:* 8005 Structural Geology: Folds and folding; 8015 Structural Geology: Local crustal structure; 8102 Tectonophysics: Continental contractional orogenic belts; 8105 Tectonophysics: Continental margins and sedimentary basins (1212); 8159 Tectonophysics: Rheology—crust and lithosphere; *KEYWORDS:* flexure, T_e, seismicity, rheology, lithosphere, collision belt, thick-skinned deformation

Citation: Mouthereau, F., and C. Petit, Rheology and strength of the Eurasian continental lithosphere in the foreland of the Taiwan collision belt: Constraints from seismicity, flexure, and structural styles, *J. Geophys. Res.*, *108*(B11), 2512, doi:10.1029/2002JB002098, 2003.

1. Introduction

[2] Two end-member hypotheses attempt to explain how mountain ranges are supported and evolve over geological times depending on the rheological model used. For instance, the classical critical wedge model considers that the topography of the orogenic belt reflects the balance between body forces arising from the deformation of homogeneous brittle wedge and the presence of basal shear stresses induced by underthrusting beneath the wedge [*Davis et al.*, 1983; *Beaumont et al.*, 1994; *Willett*, 1999]. However, the critical wedge model assumes uniform plasticity throughout the whole lithosphere, which may be an oversimplification of its mechanical behavior. The continental lithosphere is, in fact, rheologically stratified such that its strength varies with depth, as shown by experimental studies [*Brace and Kohlstedt*, 1980] and suggested by depth distribution of intraplate seismicity [*Chen and Molnar*, 1983; *Déverchère et al.*, 2001]. For example, using a vertically stratified rheology for the lithosphere, *Harry et al.* [1995] showed that major decolle-

0148-0227/03/2002JB002098$09.00

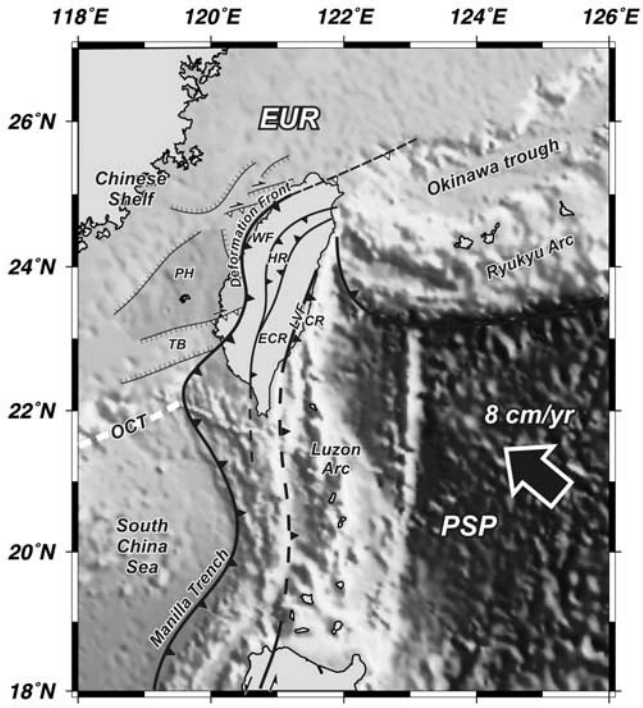

Figure 1. Plate tectonic setting at the Eurasian/Philippines Sea boundary and the arc-continent collision at Taiwan. Owing to collision obliquity the successive stages of orogenic growth are observable from southward subduction to northern postorogenic collapse. Note the presence of an inherited central high (PH) and adjacent basin (TB) in the foreland of Taiwan orogen. WF, Western Foothills; HR, Hsuehshan Range; ECR, eastern Central Range; CR, Coastal Range; TB, Tainan basin; PH, Peikang High; LVF, longitudinal valley fault; OCT, ocean-continent transition.

ments are expected in orogenic belts at midcrustal and lower crustal levels. More recently, numerical experiments of the subduction of a layered rheology continental lithosphere have emphasized how the deformation of highly contrasted rheological layers like the upper brittle crust and lower crustal ductile flow can modify the shape and long-term stability of orogens [*Burov et al.*, 2001].

[3] In agreement with critical wedge models, the Taiwan fold-and-thrust belt (Figure 1) is usually interpreted as a result of the thin-skinned tectonic wedging of Eurasian sediments deforming over a stable Eurasian lithosphere [*Suppe*, 1980, 1981; *Davis et al.*, 1983; *Dahlen et al.*, 1984]. According to the thin-skinned hypothesis, the thickest part of the Taiwan wedge should be about 20 km. However, recent works including analyses of earthquake distribution or gravity modeling have argued that the deformation within the Taiwan orogen involved the whole crust and the upper mantle [e.g., *Ellwood et al.*, 1996; *Wu et al.*, 1997]. These studies also point out the lack of evidence supporting subduction of continental lithosphere under central Taiwan; however, the authors recognize that their conclusions may be revised as our understanding of deep orogenic processes beneath the Central Range is improved. Further constraints on the deep tectonic processes were recently described by *Lin and Watts* [2002], who emphasized that additional buried loads beneath the Central Range are required to fit the observed flexure in the west foreland basin. In agreement with the model of *Wu et al.* [1997] and *Yen et al.* [1998], they proposed that the lower crust in the Central Range is overthrusting the upper crust. The departure from the initial thin-skinned model is based on observations in the Central Range, and the question of the existence and nature of a basal decollement beneath the Western Foothills (WF) is addressed. A decollement at the transition between sedimentary cover and pre-Neogene basement was initially adopted. However, recent sections across the belt front, based on interpretation of new subsurface data, have outlined that in the vicinity of inherited basement highs, the deformation involved the pre-Neogene basement [*Chang et al.*, 1996; *Hung et al.*, 1999; *Mouthereau et al.*, 2001, 2002; *Yang et al.*, 2001; *Lacombe and Mouthereau*, 2002]. To accommodate such ''thick-skinned'' deformation, a basal decollement defined by a zone of mechanical weakness should exist in the crust probably at the brittle/ductile transition in the crust. However, while the question of the rheology and strength of the Eurasian plate thus appears essential, very few works have focused on this issue. Recently, flexure modeling carried out in western Taiwan [*Lin and Watts*, 2002] indicated T_e values of 13 km for the Eurasian lithosphere. They proposed that this value is inherited from the flexural properties of the rifted Chinese margin. Unfortunately, they did not discuss how this estimate relates to the rheological layering of the Eurasian lithosphere. On the other hand, they initiated a discussion on the relations between structure, seismicity, and along-strike differences in the flexural behavior in the western foreland. Because they focused on the outer part of the basin, the problem of the link between the observed variable deformation at the belt front and plate strength was not addressed. These questions hence are still open.

[4] Our objective is to examine the layered rheology and the integrated strength of the Eurasian continental lithosphere and to discuss their relative control on variable tectonic styles and prediction of intracrustal decoupling in western Taiwan. To this purpose, we use (1) constraints from the analysis of depth distribution of earthquakes with continental geotherm and petrological data to determine the multilayered rheology of the Eurasian continental lithosphere and (2) estimates of effective elastic thickness (T_e) using an inelastic model of the deflection of the lithosphere that reflects the long-term integrated strength of the plate.

2. General Setting

2.1. Geology of Taiwan

[5] Taiwan orogen developed in response to Mio-Pliocene oblique arc-continent collision along the Eurasian and Philippine Sea plate boundary between the northern Luzon arc and Chinese continental margin (Figure 1) [*Ho*, 1976; *Suppe*, 1981]. East of the Longitudinal Valley Fault (LVF), regarded as the plate boundary, the Coastal Range (CR) represents the accreted part of Luzon arc (Figure 1). The interior of the Taiwan mountain ranges (Figure 2) comprise the exhumed Eurasian Paleozoic to Mesozoic metamorphic basement within the eastern Central Range (ECR) and Neogene to Paleogene slate belts in the Backbone Range

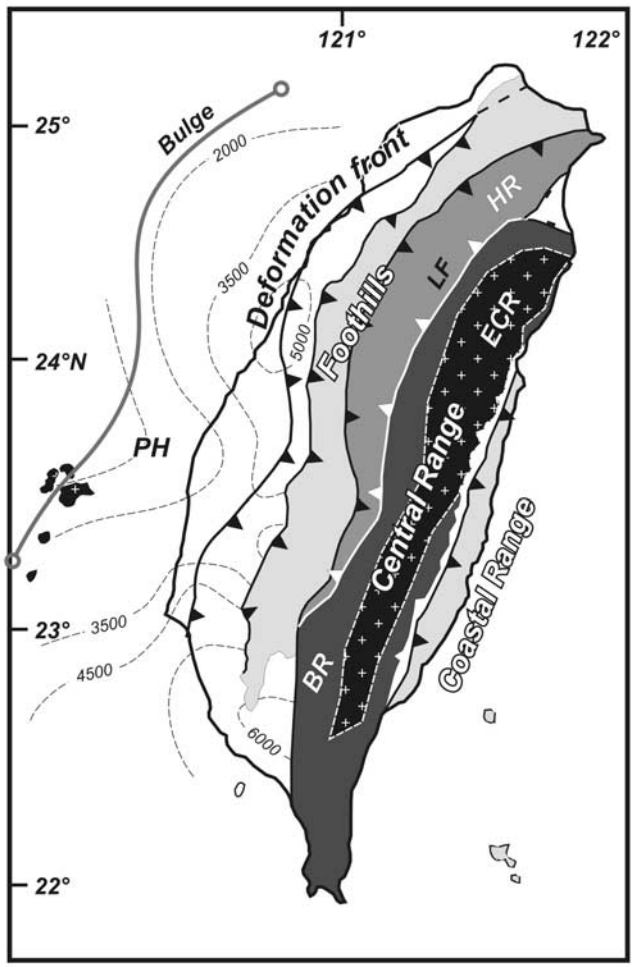

Figure 2. Main tectonic units of the Taiwan collision belt. The Paleozoic/Mesozoic metamorphic basement is exposed in the eastern Central Range. The basement is limited from the overlying slate belt of the Backbone Range (BR) by a mylonitic zone shown as white dashed line. Black dashed lines in the western foreland of Taiwan present the contoured topography of the pre-Neogene basement issued from data compiled by *Mouthereau et al.* [2002]. The position of the foreland bulge is deduced from seismic reflection data [*Yu and Chou*, 2001].

(BR) and the Hsuehshan Range (HR). Further westward, a typical foreland fold-and-thrust belt, namely the WF, is built with west verging thrust sheets of Neogene deposits. The Coastal Plain (CP) where most of the active faults concentrate makes the transition between outermost thrust sheets and adjacent foredeep. Owing to the oblique convergence between the collided continental margin oriented N60°E and the Luzon arc striking N10°E, the collision migrates southward along the Eurasian margin [*Suppe*, 1984]. Consequently, the successive stages of deformation from oceanic subduction (or incipient collision) in southern Taiwan to postcollision stage in the Okinawa trough are recognized along the strike of Taiwan where the collision culminates today (Figure 1). This progression is accompanied by the flipping of the Philippine Sea plate subduction; the oceanic plate overrides the Eurasian continental lithosphere at the latitude of Taiwan and is underthrusted beneath the Ryukyu arc northward (Figure 1). In order to avoid misinterpretations on the rheology and strength of the Eurasian continental plate due to lateral variations of the tectonic settings, our study will focus on a portion of the belt front located between latitudes 23°N and 24.5°N, where plate flexure and deformation at belt front are undoubtedly collision-related processes.

2.2. The Western Foredeep

[6] The Western flexural foreland basin of Taiwan is an isostatic response to Plio-Pleistocene emplaced thrust loads. Its geometry is constrained by the depth of the oldest sedimentary strata that form the base of the actual foredeep basin. The top of the pre-Neogene basement (a proxy of the true crystalline basement) presented in Figure 2 illustrates (1) the deflection of the basin toward the orogenic load and (2) the presence of a central high, namely the Peikang High, an oblique feature parallel to the trend of the Chinese margin. The westward extent of the foreland basin is given by the bulge position [*Yu and Chou*, 2001], which is found in close geographical correlation with the Penghu Islands of the Taiwan Strait (Figure 2). Also, it delineates a remarkable curved-shape feature concave toward the orogen, similar to the northern curvature of the orogenic front, hence outlining the relations between migrating thrust loads and the outer edge of the basin. The structure of the foreland basement is characterized by numerous half-grabens inherited from Paleogene syn-rift extensional tectonics (Figure 3). The syn-rift sediments are unconformably overlain by the Miocene postrift sedimentation. Then following the onset of the collision a prograding sequence of Plio-Pleistocene synorogenic materials was deposited unconformably onto the Miocene deposits.

2.3. Variable Structural Styles at Deformation Front

[7] Structural characteristics at the belt front are presented through three new geological balanced sections located north and south of the Peikang High (Figure 4). These sections have been balanced and restored in their precollisional situation, i.e., with respect to the Miocene layer. Irrespective of their location, restored sections clearly indicate that major thrusts originated from the inversion of inherited Paleogene normal faults of the Chinese margin. For southern sections (sections 2 and 3), subsurface data indicate that the outermost anticlines (Hsiaomei and Meilin) developed above a foreland basement uplift resulting from structural inversion of a small graben. The Meilin anticline is accounted for by a combination of thrusting within the cover and the basement. Yet northward (section 1) the frontal deformation is mostly thin skinned. If we assume that basement thickening in the upper crust is absorbed at depth within a midcrustal weak layer, the variations in the degree of basement involvement could reflect different boundary conditions at belt front, such as changes of the mechanical properties of the decoupling. Moreover, estimate of the amount of shortening gives about 20–22 km equivalent to 35–36% of shortening south of the Peikang High. Northward, where thin-skinned deformation prevails, shortening is 25% (11 km). These cross sections reveal that variations of tectonic styles are correlated with higher neogene strains and more basement deformation south of

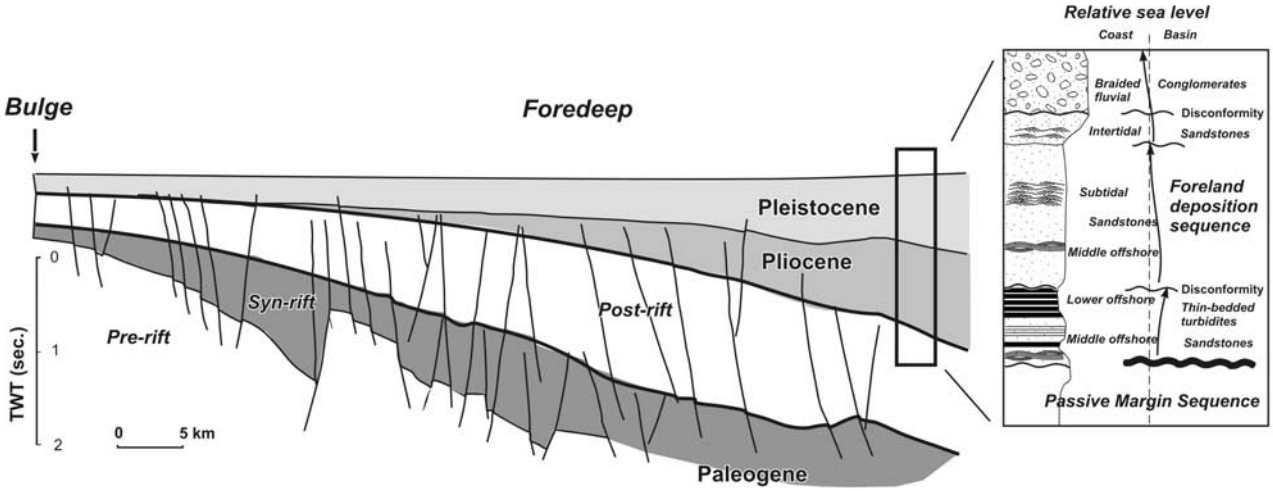

Figure 3. Cross section in the outer western foreland of Taiwan based on the interpretation of seismic reflection profile [*Yu and Chou*, 2001]. Prograding synorogenic sequences with coarsening upward strata are typically wedge shaped. Note that some Paleogene normal faults have been reactivated as normal faults in this compressional setting.

the Peikang High, possibly related to modifications of the rheology and strength of the Eurasian plate.

3. Rheology and Strength of the Eurasian Continental Lithosphere

3.1. Constraints From Seismicity and Earthquake Focal Depths Distribution

[8] Because the western foreland of Taiwan developed at an active frontal deforming zone and above a flexed continental lithosphere, seismicity can have various origins. Hence it is necessary to distinguish large earthquakes triggered by active thrust faulting at plate boundaries (interplate seismicity) from those belonging to the more long-term background record (intraplate and flexurally driven seismicity), which are more representative of the average brittle strength of the lithosphere. An example of the incidence of major frictional instabilities at the plate boundary is given by the Chichi earthquake (M_L = 7.6) which reactivated on 21 September 1999 a large fault rupture (Chelungpu fault) at the orogenic front. The moderate aftershocks and triggered earthquakes generated an increase by 100% of the number of earthquakes in 1999 and 2000.

[9] Seismicity data used in this study are issued from Central Weather Bureau Seismic Network (CWBSN), which monitors about 15,000 earthquakes each year with magnitude $M_L > 1$ (Figures 5a and 5b). Uncertainties in depth location of seismic foci are ~5 km, small enough for determination of the thickness of brittle layers. To avoid effects of large events at plate boundary we investigate a short period (1998–2001) from which the main contribution of the Chichi earthquakes (1999–2000) was extracted. The remaining records of years 1998 and 2001 (Figures 5a and 5b, respectively) are considered as representative of the secular background intraplate and interplate seismicity. The depth-frequency distribution of seismicity in the foreland is presented along a series of 70-km-long parallel profiles (Figures 5a and 5b) spaced every ~20 km and extending down to 50-km depth in the lithospheric mantle.

[10] We first distinguish in the center of the foreland a region of low seismic activity found in good correlation with the position of the Peikang basement high. By contrast, the surrounding areas of the Western Foothills and Coastal Plain exhibit high seismic activity. This indicates that the foreland basement promontory behaves as a stronger crustal portion of the Eurasian continental lithosphere, which is hardly subducting beneath the Western Foothills. Given a crustal thickness of ~30 km in the foreland [*Rau and Wu*, 1995; *Ma and Song*, 1997; *Yen et al.*, 1998], Figures 5a and 5b indicate that earthquake focal depths are essentially confined to the upper 15–20 km of the crust, with a significant peak near 10 km. Given a maximum sediment thickness of 7 km in the foreland, this suggests that the upper crustal earthquakes fall in the metamorphic basement, in agreement with basement-involved thrusting.

[11] Independently from the period considered, the total number of earthquakes per year and their frequency distribution with depth allow us to distinguish two regional subsets, one to the north (sections A and B) and the other to the south (sections C and D), where seismicity is about three times higher. One may further notice that the amount of seismicity in 2001 to the north is about twice that of 1998. Hence 2 years after the disastrous Chichi earthquake, seismicity has not returned to a ''normal'' background value. Moreover, the along-strike distribution of earthquakes in the upper crust relative to the total seismicity (Figure 6) shows that southward earthquakes shallower than 20 km represent up to 97%, while to the north this category falls in the range of 70–80%. In the lower crust the frequency of earthquakes diminishes down to the Moho depth, the mantle being essentially aseismic. This decrease is more important in southern regions, where the lower crust is almost aseismic below 20 km. By contrast, to the north, foci form a double seismogenic layer, in the upper and the lower crust separated by a thin (~5 km) nearly aseismic layer. Where thick-skinned tectonics prevails, earthquakes are limited in the upper crust; whereas northward, where it is more thin-skinned tectonics, earthquakes

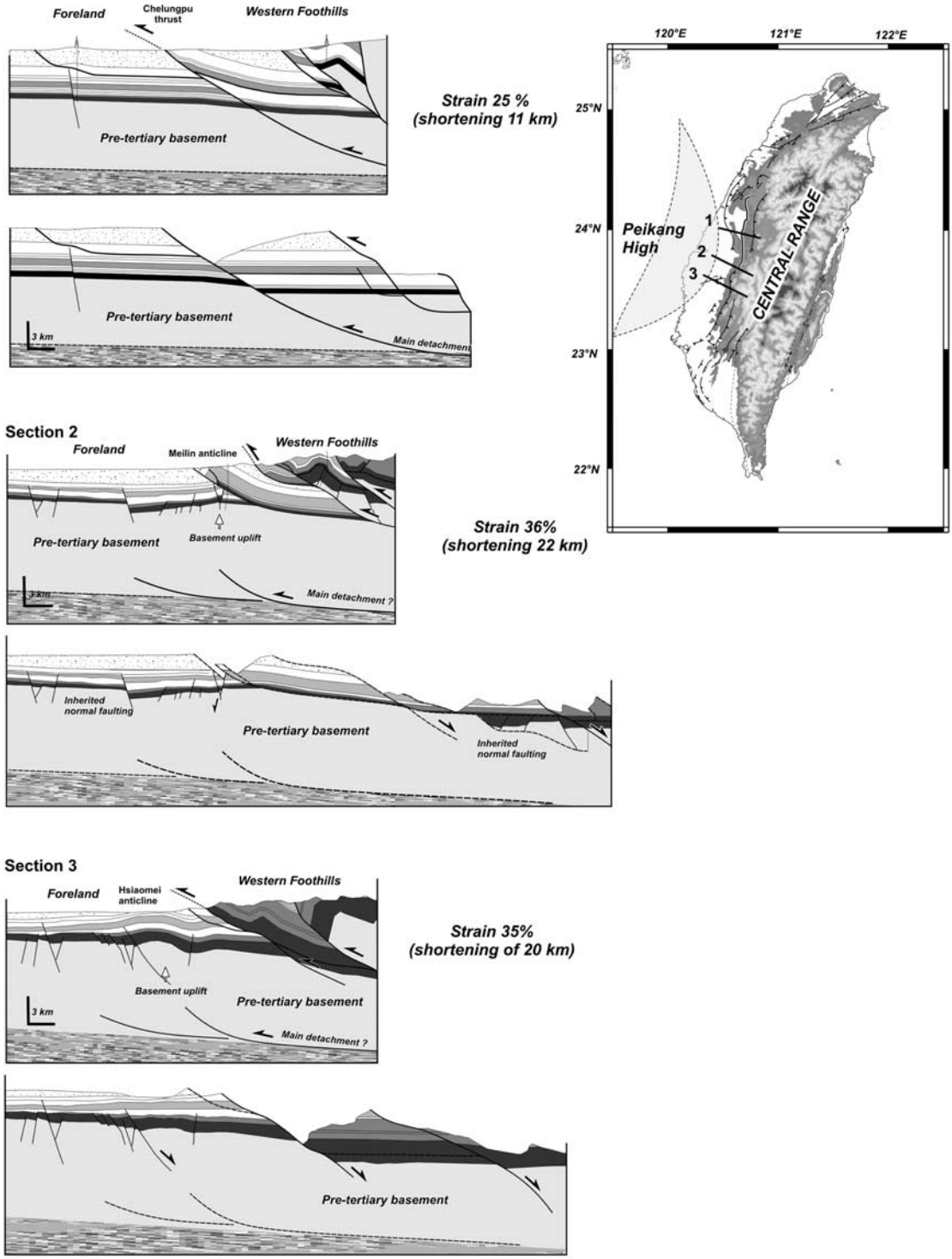

Figure 4. Balanced and restored sections across the thrust front in the western foreland thrust belt. Structural styles (thin or thick skinned) at belt front depend on the position with regard to the Peikang High. Accommodation of basement-involved deformation south of the basement high is believed to be accommodated within a midcrustal detachment defined by the less competent crustal layer.

occur throughout the crust. These observations reveal that the crustal seismicity is neither distributed homogeneously nor randomly in Eurasian plate but rather follows the spatial variations of tectonic styles in the vicinity of the Peikang High.

3.2. Continental Geotherm

[12] In this section, a preliminary temperature-depth profile of the continental lithosphere is calculated using a plate cooling model (Figure 7 and Table 1). We assume that the thermal structure of the Eurasian lithosphere in

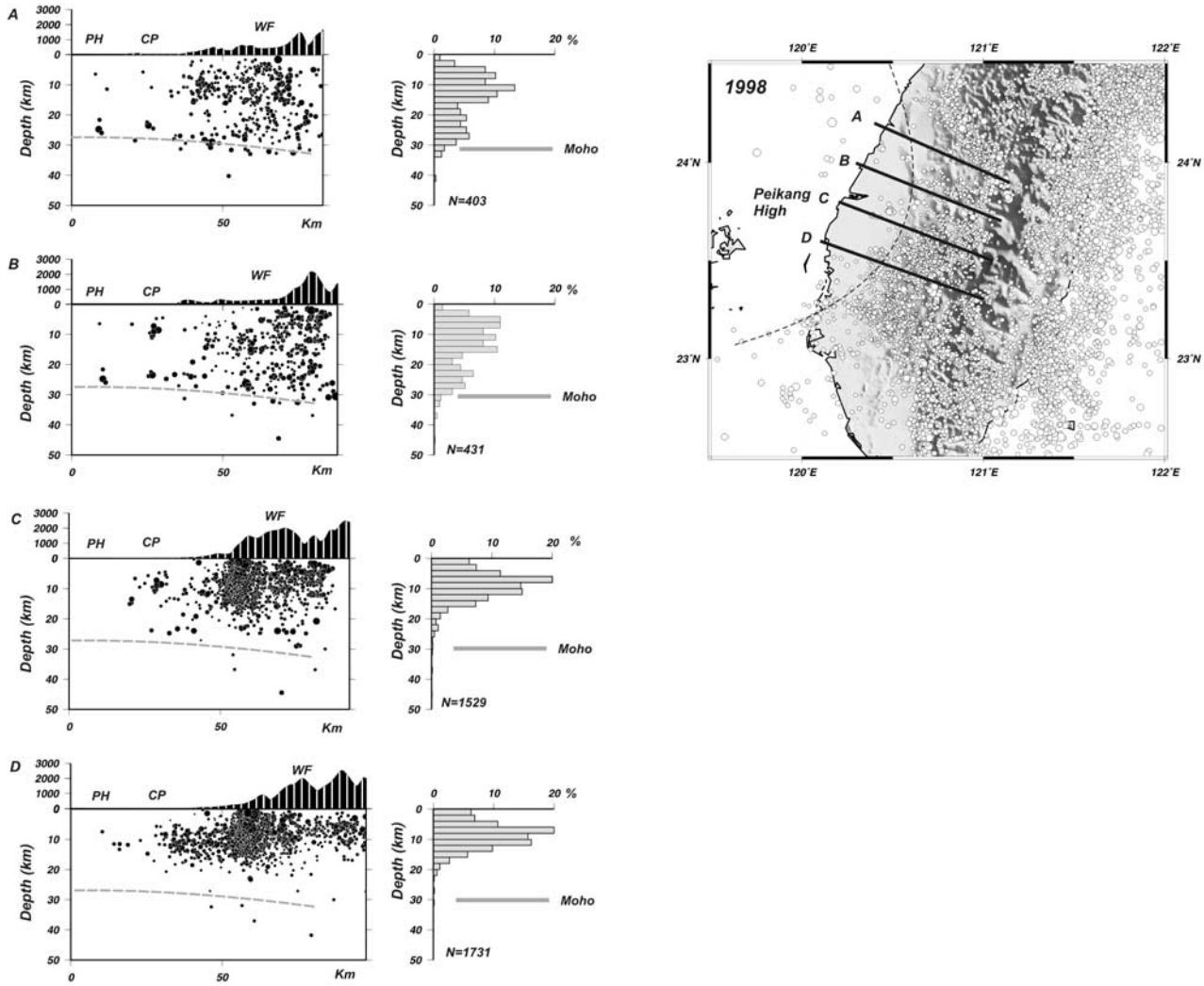

Figure 5a. Depth-frequency distribution of the 1998 yearly record of earthquakes (magnitudes $M_L > 1$) within the Eurasian crust of the western Taiwan foreland. Data are issued from the CWBSN catalog. Four 70-km-long seismic profiles (A–D) are investigated through (left) depth distribution of earthquakes and (right) depth-frequency distribution of seismic events. The amount of earthquakes selected are shown at the bottom of each histogram. Note the concentration of shallow seismicity in sections C and D south of the Peikang High (PH) in association with higher topography. Note also that the lower bound of the crustal earthquakes delineates a plane deepening 5° toward the interior of the mountain range, fitting with the Moho deflection.

foreland area can be approximated by a steady state model. The thermal age is defined as the point from which the lithosphere has initiated its cooling. In the case of the Chinese continental margin, the last thermal event which has led to a complete thermal resetting coincides with the initiation of oceanic spreading in the South China Sea during the late Oligocene, i.e., ~32 Ma [e.g., *Lee and Lawver*, 1995]. Unfortunately, the thickness of the Eurasian lithosphere remains unconstrained in western Taiwan, we hence consider an average thickness of ~120 km. Additional control on the consistency of our results is given by the generally high 80–100 mW m^{-2} heat flow in the western foreland, constrained by geothermal logs penetrating to Tertiary sediments in several oil fields [*Suppe and Wittke*, 1977; *Barr and Dahlen*, 1990]. We compare the observed heat flow and the values of heat flow predicted by the model. We assume homogeneous thermal conductivity and diffusivity for the whole lithosphere (Table 1). The surface temperature T_0 is fixed to 0°C, and T_m at the base of continental lithosphere (1330°C for dry peridotite at upper mantle pressure) is fixed.

[13] Without any other heat sources we compute surface heat flow of ~80 mW m^{-2}. The consistency of our results with the measured heat flow indicates that other contributions to the total heat flow should be minor. However, it is well known that for continental crust, radiogenic heat production is a major contribution to surface heat flow. To this respect, a maximum contribution of 20 mW m^{-2} is able to fit the upper bound of the observed heat flow. Computations reveal that heat production of an average dioritic crust can fit the observed heat flow while more classical Qz-dominated crust cannot. From above, other

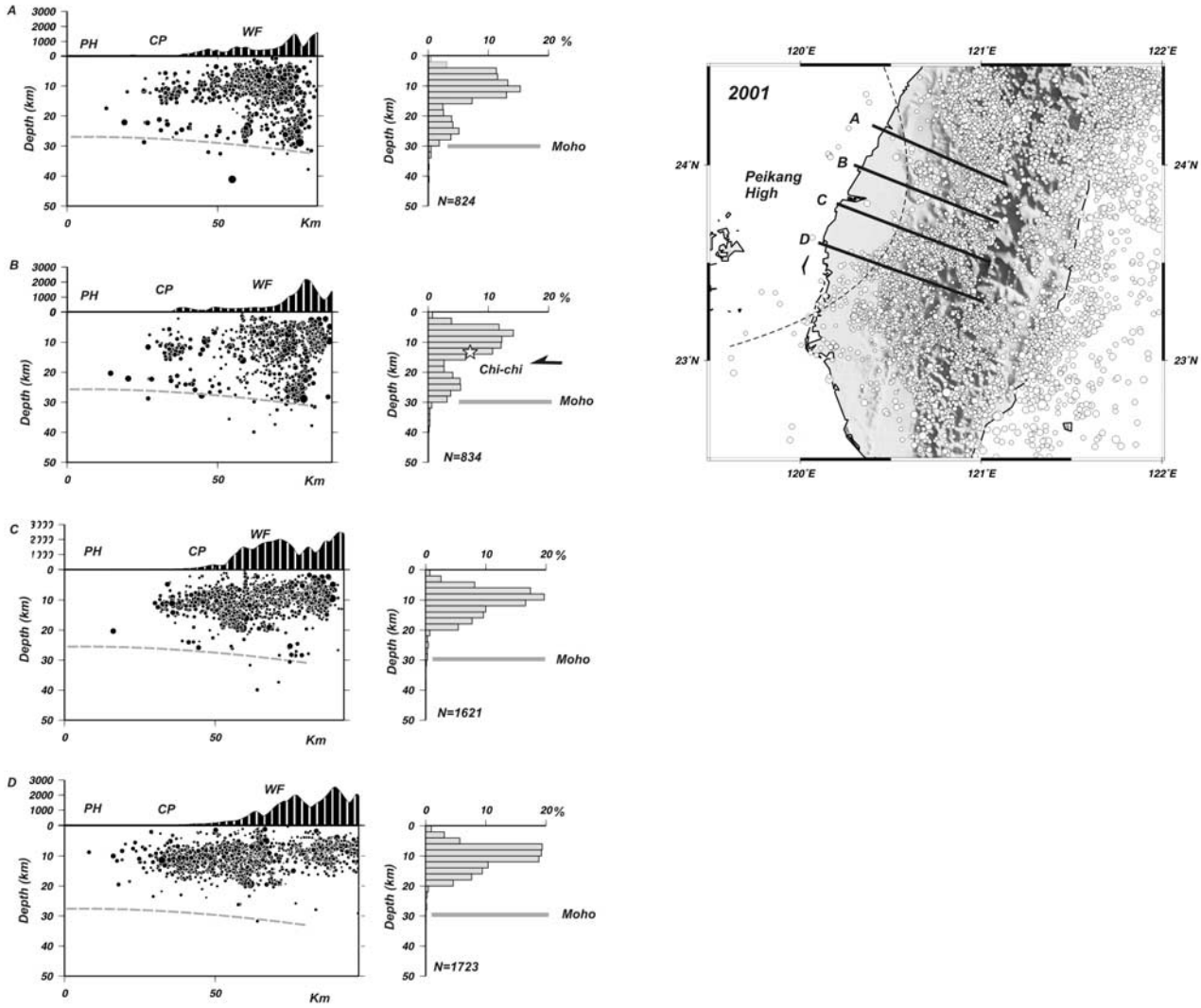

Figure 5b. Same study as for Figure 5a but for the 2001 yearly record. The small star beneath the Western Foothills corresponds to the approximate focal depth of the 21 September 1999 Chichi earthquake.

effects, such as thermal blanketing, able to considerably reduce the strength of continental plate [*Ziegler et al.*, 1998] are here attenuated because of limited syn-rift and postrift sediments accumulation (~2–3 km) on the margin.

[14] The resulting geotherm (Figure 7) indicates temperatures of 400°C at 15 km and pressures of ~0.4 GPa for a lithostatic pressure of about 27 MPa km^{-1} (for an average density for crust and sediments of 2,7). At the Moho, temperature reaches ~800°C and pressure is approximately 0.8 GPa. Such *P-T* conditions predict greenschists facies for middle crust and granulite-type metamorphism for lower crustal material with intermediate (dioritic) or more mafic (gabbroic) bulk composition. Such HT/LP gradient with crustal geotherm of 30°C km^{-1} is significantly higher than the "normal geotherm" of 20°–25°C km^{-1}. This geotherm indicates a hot Eurasian continental crust with mafic characteristics.

3.3. Strength Profile

[15] In this section we aim to compute synthetic yield stress envelopes for the Eurasian lithosphere that best

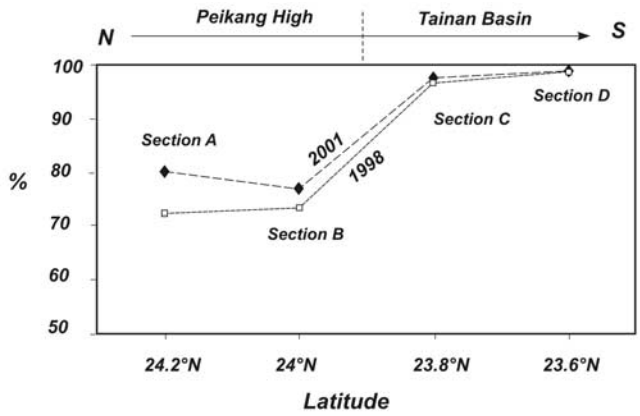

Figure 6. Percentage of earthquakes in the upper crust <20 km along strike of orogen as a function of position (latitude). Data used are the same as in Figures 5a and 5b. Note the slight increase of seismicity between 1998 and 2001 northward induced by the Chichi earthquake.

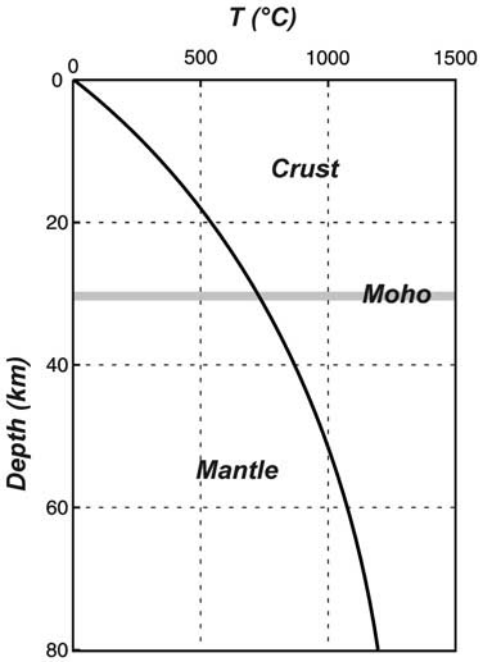

Figure 7. Geotherm within the Eurasian continental lithosphere. A plate cooling model is used (see Table 1).

account for the thickness and location of seismogenic layers and geotherm and petrological data. This profile is believed to represent the averaged layered rheology of the Eurasian lithosphere in the central portion of the Taiwan foreland where collision occurs.

[16] Drillings in the Peikang Plain have revealed the presence, within the pre-Neogene basement, of Eocene to Cretaceous arkoses, with local HT/LP paragenesis indicating the presence of plutonic intrusion [*Chiu*, 1973] that is correlated offshore in the Penghu Islands with Miocene intraplate basaltic volcanism. Consequently, the upper crust in the foreland appears to be a combination of quartz-rich metasediments and mafic metamorphic intrusive rocks corresponding to a granodiorite-type composition.

[17] The conditions for brittle failure in the lithosphere are independent of rock type and temperature but are strongly controlled by pressure [*Byerlee*, 1978]. The brittle strength can be approximated by the Sibson's formulation [*Sibson*, 1974] for which the coefficients of friction and cohesion for prefractured rocks are equal to internal friction and cohesion for intact samples: $\sigma_1 - \sigma_3 = \beta\rho g z(1 - \lambda)$, where $\sigma_1 - \sigma_3$ is the differential stress, z is the depth, ρ is the average density of the overburden, g is the acceleration of gravity, β is a coefficient which depends on the type of faulting, and λ is the pore fluid ratio. For hydrostatic pressure, λ is 0.36, and it is 0 and 0.7 for dry and wet conditions, respectively. Even though this formulation constitutes a lower bound for the failure of most rocks, in situ stress measurements made in deep boreholes have indicated that the strength of continental crust is essentially limited by the friction on favorably oriented preexisting fractures with nearly hydrostatic pore pressure gradient [*Zoback and Healy*, 1992; *Brudy et al.*, 1996]. For comparison, a high fluid pressure ratio λ of 0.65 has been estimated from geophysical logging of wells near the Taiwan deformation front [*Suppe and Wittke*, 1977]. Such overpressured domain is confined to the upper sedimentary level, i.e., <2–3 km, where lithostatic pressure is low and cannot be considered as relevant for the whole crust. Consequently, we adopt more reliable hydrostatic conditions for the brittle profile.

Table 1. Physical Parameters Used for Modeling the Continental Geotherm of Figure 7

Symbol	Definition	Value
T_L	lithosphere thickness	120 km
T_c	crust thickness	30 km
κ	thermal diffusivity	0.83×10^{-6} m^2.s^{-1}
K	thermal conductivity	2.5 W.m^{-1} K^{-1}
ρH_c	heat production for Diorite	0.5×10^{-6} W.m^{-3}
t	thermal age	32×10^6 an
T_0	surface temperature	0°C
T_m	asthenospheric temperature	1330°C

[18] When deviatoric stresses and temperature are high enough the rocks may fail by ductile creep flow. Laboratory experiments have indicated that the flow for most rocks and minerals of the lithosphere results from a thermally activated dislocation creep process [e.g., *Brace and Kohlstedt*, 1980]. The deviatoric stresses for dislocation creep follow a power law given by $\Delta\sigma = (\varepsilon/A^*)^{1/n} \exp(H/nRT)$, where n is the stress component, A^* is a material constant, H is activation enthalpy, $R = 8.314$ J mol^{-1} K^{-1} is the gas constant, and T is the temperature in Kelvin (Table 2) [*Goetze*, 1978; *Hansen and Carter*, 1982; *Wilks and Carter*, 1990].

[19] The distribution of focal depths of earthquakes in the western foreland can be interpreted in the light of mechanical strength profiles determined from rock mechanics experiments. Seismicity in continental areas is frequently associated with the upper crust, while the lower crust is usually too weak to have remarkable brittle strength [*Chen and Molnar*, 1983]. The transition between brittle and ductile regimes in the crust predicted by the strength profile (Figure 8) is expected at 12–15 km, values agreeing with the observed cutoff depth of crustal seismicity (Figures 5a and 5b). Despite local discrepancies in the density of earthquakes in the lower crust it appears that, more regionally, below 12–15 km the crust can remain seismogenic. The seismicity in the lower crust can be explained [*Cloetingh and Burov*, 1996] by (1) a change in the crustal composition with a more "basic" (diabase, diorite) composition at depth with a high temperature of creep activation; (2) localized strain rate acceleration along deeply penetrating faults, which can keep the Qz-controlled material brittle [e.g., *Déverchère et al.*, 1993]; and (3) changes in water content [*Maggi et al.*, 2000].

[20] The classical Qz-dominated composition of the crust here fails to account for the seismicity observed down to depths of 15 km. On the basis of petrological observations and a continental geotherm, a granodioritic composition

Table 2. Parameters of Dislocation Creep for Lithospheric Rocks and Minerals Adopted for Computation of Yield Stress Envelops[a]

Layer	Rheology	A, Pa^{-n} s^{-1}	H, kJ mol^{-1}	n
Upper crust	quartz-diorite (dry)	1.2×10^{-16}	212	2.4
Lower crust	mafic granulite (dry)	8.8×10^{-22}	445	4.2
Mantle	olivine (dry)	7×10^{-14}	520	3

[a]See references [*Goetze*, 1978; *Hansen and Carter*, 1982; *Wilks and Carter*, 1990].

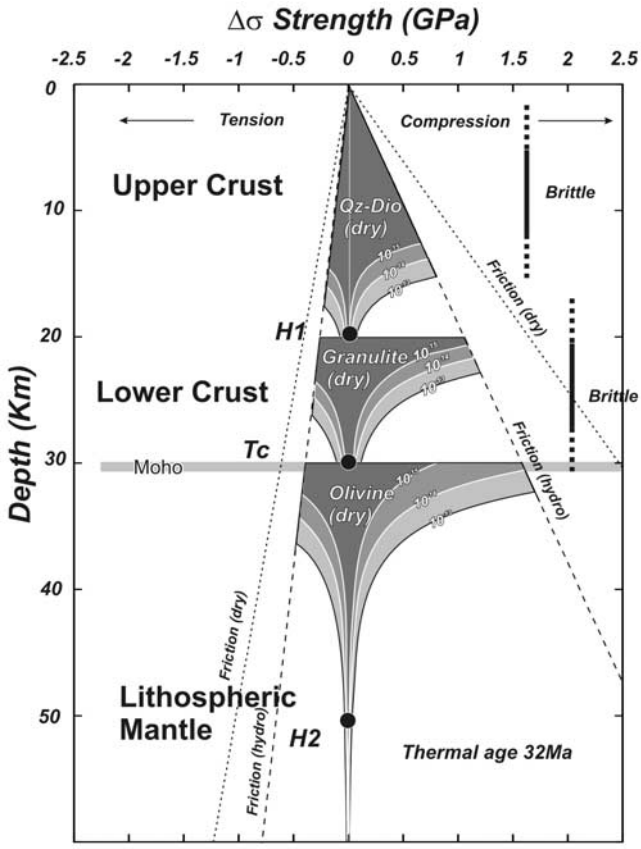

Figure 8. Yield-stress profiles within the Eurasian plate for strain rates from 10^{-13} to 10^{-15} s^{-1}. Crustal composition adopted is Qz-diorite in the upper crust, mafic granulite in the lower crust, and olivine for the mantle. Solid circles correspond to depths of mechanically strong layers inferred from the strength profile. The range of brittle deformation is deduced from the analysis of depth distribution of earthquake foci (Figures 5a and 5b).

approximated by Qz-diorite rheology with higher temperature of creep activation more reliably represents the upper crust (Figure 8). Considering the present-day convergence rate at Taiwan of 7 cm yr^{-1} from NUVEL-1 [*Seno et al.*, 1993] or 8 cm yr^{-1} deduced from GPS data [*Yu et al.*, 1997] the average strain rate across the mountain belt is about $3–5 \times 10^{-15}$ s^{-1}. These values are consistent with geological strain rates of $2.5–3.5 \times 10^{-15}$ s^{-1} since 5 Ma at the belt front derived from balanced cross sections (Figure 4). In the following, plastic failure curves are computed for strain rates ranging from 10^{-13} to 10^{-15} s^{-1}, providing lower and upper bounds for calculation of creep laws of rocks and minerals.

[21] The most common lithologies for the lower crust (diabase or Qz-diorite) here failed to reproduce, even for high strain rates, sufficient brittle strength to explain earthquakes. The best solution is for a granulitic composition allowing high deviatoric stresses to be sustained below 12–15 km, hence explaining part of the seismicity observed along northern profiles (Figures 5a and 5b). The mantle is dominantly olivine. The resulting profile predicts long-term strength for the upper Eurasian mantle. However, the seismicity distribution in the foreland reveals that the upper mantle is nearly aseismic for both the northern and southern profiles. An explanation is the lack of sufficiently high stress [*Watts and Burov*, 2003] to produce fracture of mantle material, i.e., in the Taiwan case ~1.5 GPa (compression). Furthermore, in order to exceed this stress the required force should be an order of magnitude higher than any plate dynamic forces for the whole lithosphere.

4. Lithosphere Flexure and T_e Estimate

[22] In this study we used gravity data from the work of *Hsu et al.* [1998], who compiled data from shipboard [*Liu et al.*, 1992], onland [*Yen et al.*, 1990], and satellite-derived data [*Sandwell and Smith*, 1997]. Sediment-corrected Bouguer anomalies are deduced from free-air anomalies by extracting density contributions of topography, sediments, and water. The final grid resolution is about 1′-1′ (Figure 9). The Bouguer gravity data reveal a regional positive anomaly of +20 mGal in the bulge area, west of the foreland basin, probably enhanced by magmatic crustal underplating, as suggested by the existence of intraplate magmatism. Before modeling of the basin flexure, in terms of calculated Bouguer anomalies of the deflected Moho, and in order to compare with calculated Bouguer anomalies of the Airy model, we have subtracted 20 mGal from the observed Bouguer anomalies.

[23] Spatial distributions of Bouguer anomalies (Figure 9) outline the general pattern of the Taiwan arc-continent collision. To the east, the highest positive anomalies of +200 mGal correspond to denser oceanic crust of the Philippine Sea plate and contiguous Luzon volcanic arc. In western foreland, anomaly lows related to the downward deflection of the lithosphere and the Neogene sedimentary infill trend more or less parallel to the orogen and mimic the base of the pre-Neogene basement (Figure 2). A central gravity high in the foreland corresponding to the Peikang basement high is flanked northward and southward by two gravity lows showing two Neogene foredeeps.

[24] To determine T_e we use a semianalytical approach developed [e.g., *Burov and Diament*, 1995] to model the deflection of a lithosphere caused by distributed loads (topography) and horizontal and vertical forces acting at a plate boundary. During loading, deflection of an inelastic plate is modeled as deflection of an equivalent elastic plate with variable T_e. The lithosphere material behaves elastically as long as the imposed stresses do not reach the yield strength. If the bending stresses within the plate, due to the bending of a plate, exceed the yielding limits, inelastic (brittle or ductile) deformation occurs. Because of nonlinearity, T_e varies in space as a function of increasing plate curvature. T_e will be more reduced at the edge where the effect of plate interaction is the maximum. The calculated T_e also largely depends on the position of rheological interfaces within the rheologically layered plate, which is not taken into account in more classical flexure modeling that assumes elastic behavior for the plate. T_e of a layered plate is estimated through a nonlinear function [*Burov and Diament*, 1995] $\tilde{T}_e = \tilde{T}_e(\Phi)$ such that

$$\tilde{T}_e^3 = \frac{\tilde{D}(\Phi)}{D_0} = \frac{-\tilde{M}_x(\Phi)R_{xy}}{D_0} = \frac{\tilde{M}_x(\Phi)}{D_0}\left(\frac{\partial w(\Phi)^2}{\partial x^2}\right)^{-1},$$

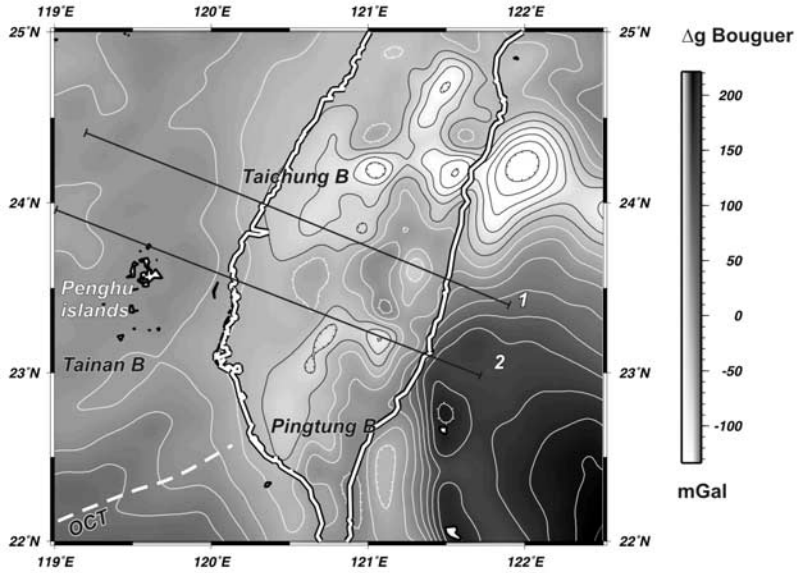

Figure 9. Bouguer anomaly map (1′-1′ grid) of Taiwan after data compiled by *Hsu et al.* [1998] and location of profiles used for the flexure modeling. Foreland gravity lows and highs in western Taiwan well correlate with the occurrences of flexural basins (Taichung and Pingtung basins) and a basement topographic high in the Penghu Islands, the Peikang High.

where $D_0 = E[12(1 - \nu^2)]^{-1}$ is the initial rigidity, $R_{xy} \approx -(w'')^{-1}$ is the radius of plate curvature, $w(x)$ is the vertical deflection of the plate, and $\bar{M}_x$ is the bending moment.

[25] The nonlinear feedback between local strength and plate structure is solved by an iterative numerical approach. The plate rheology is simply described by three parameters which reflect the brittle-elastic-ductile plate rheology used and correspond to the base of competent layers, $H1$ (depth of brittle/ductile transition in the crust), T_c (Moho depth), and $H2$ (bottom of the mechanical lithosphere). These values are defined as the depths at which the yielding strength does not exceed 1–5% of the lithostatic pressure. The input thickness of competent layers corresponds to those best accounted for by the yield stress profiles shown in Figure 8. Accordingly, one initially sets T_c, $H1$, and $H2$ to 30, 20, and 50 km, respectively, for Eurasian lithosphere. We then slightly modified the depths of these interfaces in order to better adjust the lithospheric deflection to observed gravity data.

[26] Forward flexure modeling, in terms of Moho gravity output, was carried out for two 300-km-long profiles located in the central portion of the foreland (Figure 10). The density contrast used to compute Bouguer anomalies only refers to crust and mantle (Table 3). Profiles are taken parallel to the average convergence direction, ~340°N, and perpendicular to the trend of main topographic and thrust loads. We do not attempt here to reproduce gravity anomalies in the Central Range but rather focus on the foreland flexure. For each profile, we first computed the theoretical Bouguer gravity resulting from a local, Airy-type compensation of the topographic load. Then T_e estimates are made by fitting the gravity signal output from the deflected Moho to the observed gravity data. Plate deflection is produced by applying on the edge of the plate both the effect of topographic load and bending moments representing the cumulative effects of buried loading and horizontal forces. Several tests have been performed for both profiles using different applied bending moments and different positions for the loads. Because T_e is variable, i.e., maximum at the bulge and then decreasing as the curvature increases, solutions for T_e are given as upper and lower bounds (Figure 10 and Table 4).

[27] On the basis of geological arguments and tomography data, break off or delamination of the continental lithosphere is usually invoked to explain the flipping of subduction from south to north [*Teng et al.*, 2000; *Chemenda et al.*, 2001; *Lallemand et al.*, 2001; *Malavieille et al.*, 2002]. Moreover, because of the lack of geophysical evidence for continental subduction, at least in central Taiwan [*Wu et al.*, 1997], the continuity of the plate flexure beneath the Central Range is questionable. *Lin and Watts* [2002] also demonstrated that the hypothesis of a continuous plate is unable to explain the observed flexure. A 2-D broken plate model hence appears more representative of the collision setting. The position of the plate break is however much more problematic. *Lin and Watts* [2002] argued that the most likely position for a plate break is along the Longitudinal Valley, which is the plate suture in between Eurasia and the Philippine Sea plates. However, from arguments listed above, there are major restrictions for this possibility, at least in central Taiwan. Another major restriction concerns the relative displacement along the plate suture. The Central Range is presently uplifted at higher rates than the Coastal Range [e.g., *Chen*, 1984]. This implies a normal motion along the plate suture and not reverse as would be expected. Consequently, in the collision domain, the deformation and flexure within the Eurasian lithosphere cannot be easily related with thrust loads of the Philippines Sea plate. An alternative is to hypothesize that

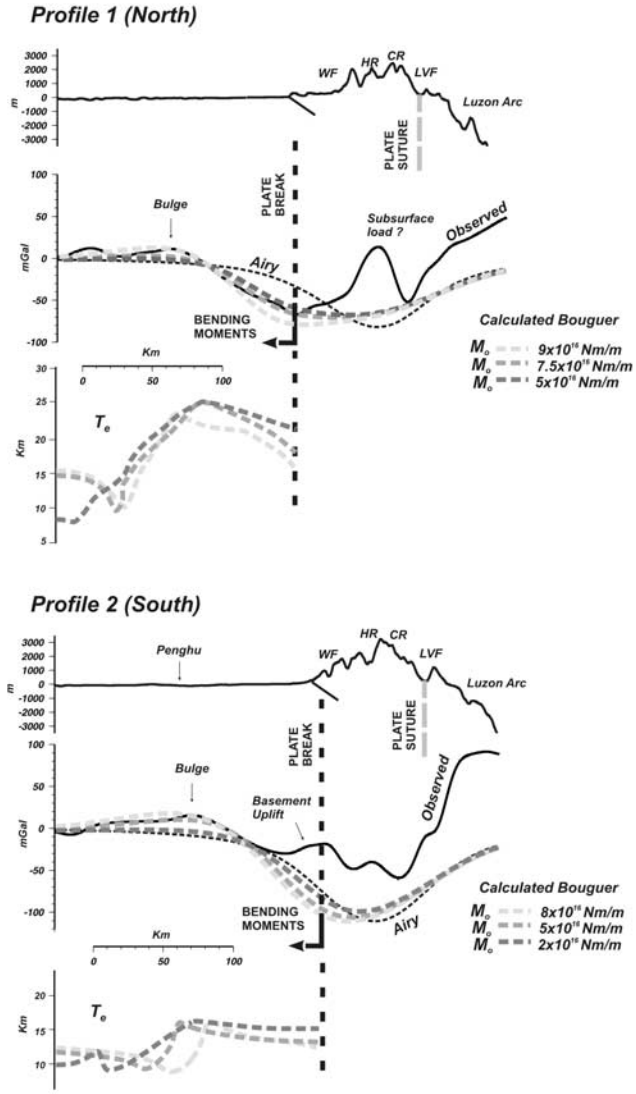

Figure 10. Comparison of observed (black solid line) and calculated Bouguer gravity anomalies (gray dashed lines) along two profiles north (top) and south (bottom) across Taiwan (location in Figure 9). The anomaly calculated assuming local Airy isostasy is also presented. Spacing between lines is about 35 km. Flexure models (in terms of gravity signal output) are based on a broken plate model, with a rheology defined in Figure 8. Estimations of T_e use an inelastic model [*Burov and Diament*, 1995]. The T_e profiles obtained for both northern and southern profiles are plotted below corresponding flexure modeling. The plate is subject to topographic load and different additional bending moments.

the plate flexure is a result of a combination of vertical and horizontal loads acting at the eastern edge of the observed foreland basin, i.e., beneath the Western Foothills. An argument supporting this hypothesis is the density of crustal seismic activity and compressional mechanisms observed in the Western Foothills and Coastal Plain which likely represents intracrustal thrust loads at the edge of the plate (Figures 5a and 5b). We hence decided to test in the flexure modeling a plate break located at the belt front. An advantage of this choice is that the basement flexure is modeled only where it is observed and the flexure is not extrapolated beneath the Central Range where tectonic processes are unconstrained.

[28] To the north (profile 1) in central Taiwan the positive Bouguer anomalies are higher than predicted by the Airy model (Figure 10). This was interpreted as due to the presence of buried loading beneath the Central Range [*Lin and Watts*, 2002]. By contrast, in the western foreland, the Airy Moho is higher than the observed Bouguer anomalies. This classical gravity "low" in the Taichung basin, filled with synorogenic sedimentation (Figure 2), reflects flexural compensation on the side of the orogen. Southward (profile 2), a similar discrepancy between Airy and observed Bouguer anomalies is observed in the Central Range, indicating under compensated topography. Westward, the relative better agreement between the Airy model and the observed Bouguer anomalies with respect to northward is probably explained by the presence of the Peikang basement high.

[29] For both profiles, the flexure model reveals that the best position for plate break is located in the vicinity of the thrust front. One further observes that the westward advance of the point of application of the load for profile 1 with respect to profile 2 is correlated with a nearly similar displacement of the bulge into the foreland. This evolution is best accounted for by vertical buried loads and/or horizontal forces arising from plates interaction. Estimation of T_e reveals similar values for both profiles ($\sim$10 km) in the backbulge domain, whereas eastward, in the foredeep domain, where curvature increases, different estimates of T_e are obtained (Figure 10 and Table 4). Along the northern profile (profile 1), T_e range from 17 km at the leading edge to 25 km at the bulge, whereas southward (profile 2) lower values ranging in between 13 and 16 km are obtained.

[30] The estimated T_e values of $\sim$15–20 km are consistent with other flexure modeling using elastic plate model with constant T_e [*Lin and Watts*, 2002]. However, the use of a realistic brittle-elastic-ductile plate rheology enables the observed flexure to be accounted for by loads acting near the deformation front. These values can be first interpreted as indicative of the thermal state of the rifted Chinese margin inherited from the Oligocene spreading in the South China Sea. However, other mechanical properties such as the degree of crust/mantle coupling and the stress/strain distribution can also be invoked. The obtained T_e values predict decoupling between crust and mantle, with reduction of 50% from a coupled one for which T_e should be about 40–50 km. The inferred depth of rheological interfaces $H1$ and $H2$ (Table 4) indicates that the thickness of the competent crust ($\sim$15–20 km) is comparable or greater than the thickness of the competent mantle lithosphere ($\sim$10–20 km). This indicates that the integrated strength

Table 3. Parameters Used in the Flexural Modeling

Symbol	Definition	Value
ρ_m	mantle density	3300 kg m^{-3}
ρ_c	crustal density	2670 kg m^{-3}
g	gravitational acceleration	9.81 m s^{-2}
G	gravitational constant	6.67×10^{-11} m^3 kg^{-1} s^{-2}
E	Young modulus	65×10^9 Pa
ν	Poisson's ratio	0.25

Table 4. Mechanical Parameters Deduced From Flexural Modeling[a]

Parameters	Name	Profile 1	Profile 2
T_e	effective elastic thickness	17–25 km	13–16 km
D	rigidity	4.3×10^{22}–1.4×10^{23} N m^{-1}	2–3.6×10^{22} N m^{-1}
M_0	bending moment	7.5–9×10^{16} Nm m^{-1}	5–8×10^{16} Nm m^{-1}
T_c	crustal thickness	30 km	30 km
$H1$	base of the MSC	20 km	15 km
$H2$	base of the MSL	50 km	40 km

[a]Values of T_e and rigidity obtained along gravity profiles 1 and 2 (Figure 9) are shown with applied bending moments and position of rheological interfaces. MSC, mechanically strong crust; MSL, mechanically strong lithosphere.

of the lithosphere is essentially controlled by the strength of the crust and not by the mantle.

5. Discussion

[31] Apart from the observations of regionally similar flexural properties of the Chinese margin we, nevertheless, show that lower T_e values southward indicate a reduction of plate rigidity. Also, flexure modeling indicates that lower T_e is correlated with a reduced thickness of the mechanically strong crust and mantle (Table 4). Assuming that the thermal state and lithospheric rheology are similar for both profiles, the most likely possibility for the reduction of the plate strength is that the plate preferentially yields south of the basement promontory. This could be explained by higher plate curvature, which is related to bending stresses and/or additional in-plane tectonic stresses at the plate boundary. Hereafter, we examine these two possibilities.

[32] The average dip angle defined by the observed basement deflection (Figure 2) leads to estimate a plate curvature of $\sim 1.2 \times 10^{-6}$ m^{-1}, equivalent to a radius of $\sim$841–864 km, slightly increasing southward. Using these values we deduce nearly similar bending stresses of $\sim$80 MPa km^{-1} for both profiles within the elastic portions of the yield stress envelops (Figure 11). The convex upward bending of the layered continental lithosphere leads to brittle extensional failure in the upper 10 km of the crust, in agreement with evidences of Plio-Pleistocene normal faulting in the outer foreland (Figure 3) and occurrences of extensional focal mechanism of earthquakes offshore in the Taiwan Strait [e.g., *Kao and Wu*, 1996]. At the base of the crust, the plate bending leads to compressional ductile flow, providing an explanation of the crust/mantle decoupling within the lower crust as predicted by T_e estimates. However, the bending stresses are still elastically supported at depths of $\sim$10–15 km, which contradict the observation of active brittle faulting at such depths (Figures 5a and 5b). Moreover, focal mechanisms in this area reveal a combination of right-lateral strike-slip and reverse faulting compatible with N120°E compression [*Rau and Wu*, 1995; *Wu et al.*, 1997], which is indicated by high-angle thrust faults along balanced geological sections (Figure 4). However, while the bending stresses can explain part of the structural observations in the outer foreland, they fail to reproduce the along-strike variations and reduction in T_e as well as the observed distribution of seismicity and compressive mechanisms in regions close to the deformation front.

[33] We now examine the implications of additional in-plane stresses across the plate boundary. Estimates of Neogene differential stresses of $\sim$60–145 MPa in the vicinity of the thrust front [*Lacombe*, 2001] indicate that even shallow (<2 km) compressional stresses are high enough to overprint flexurally controlled extension in the upper crust (Figure 11). More realistic lithospheric-scale tectonic stresses equal to $\sim$500–700 MPa arising from plate coupling are able to cause compressional brittle deformation down to 12 km in the upper crust (Figure 11). This level of stress can be locally higher, e.g., because of locally more frontal collision, and hence explain part of the observed variations of the seismicity. However, it is still unable to predict brittle faulting deeper in the lower crust where high

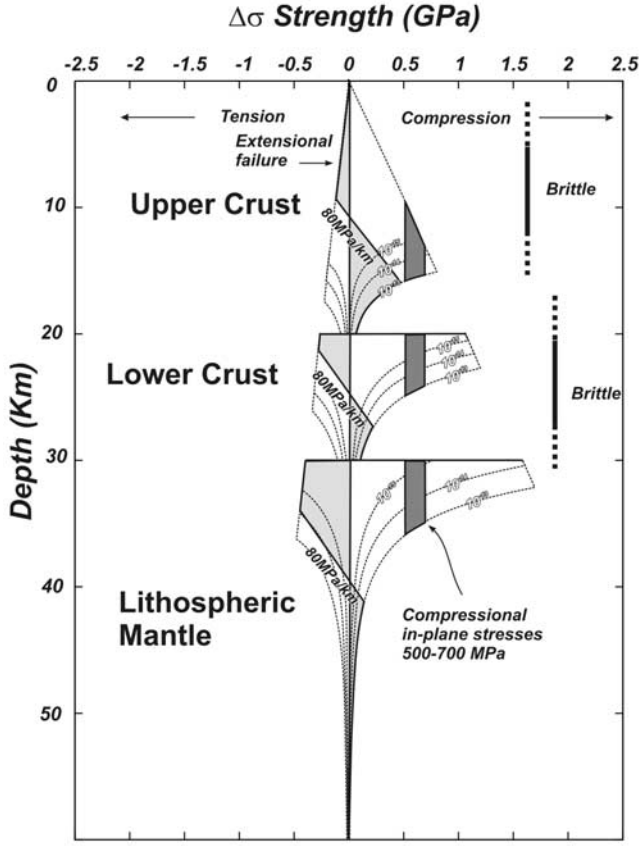

Figure 11. Distribution of bending stresses within the Eurasian continental using similar plate rheology of Figure 8. Elastic portions appear in gray. Concave upward bending of the lithosphere leads to extensional faulting in the upper crust, as seen in Figure 3, and upper mantle. In the lower crust, stresses lead to ductile flow and decoupling of crust and mantle. Compressional in-plane stresses at plate boundary on the order of 500–700 MPa can eliminate the extensional faulting in the upper crust and explain crustal seismicity down to 12 km.

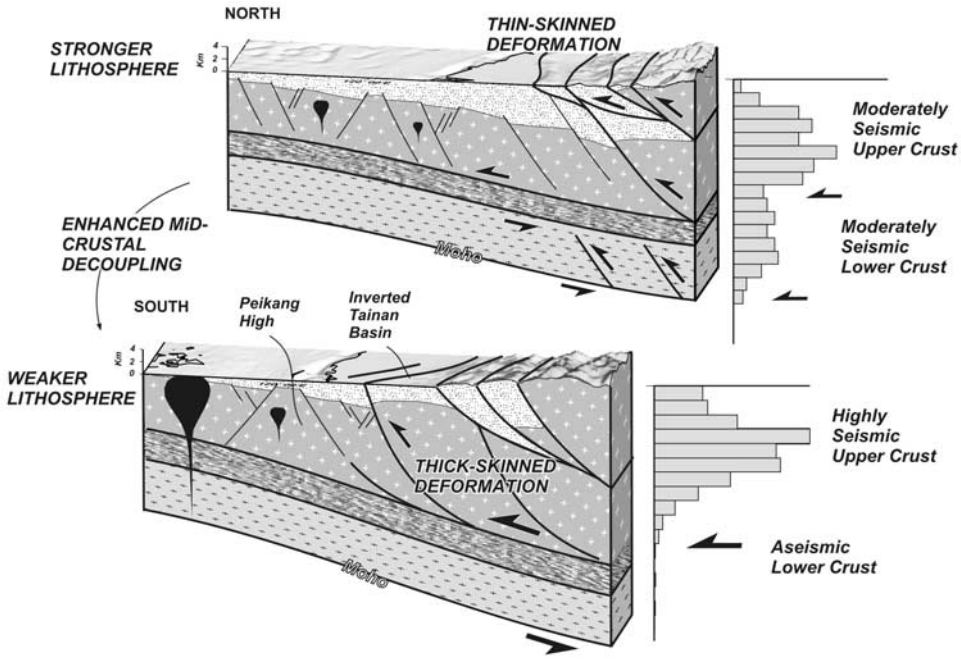

Figure 12. Three-dimensional bloc diagrams of the Taiwan foreland showing relationships between variations of structural styles (thin or thick skinned) and the strength of the deflected Eurasian plate. Depth-distribution of earthquakes for both regions reveals different mechanical behavior in the crust related to the distribution of brittle stresses and strain rates. Black arrows on histograms represent expected positions of crustal decoupling. The size of the arrows is proportional to their relative importance. This figure resumes the role of enhanced midcrustal decoupling in reducing the integrated strength of the Eurasian lithosphere.

stresses of ~1 GPa are required. Other mechanisms, such as local acceleration of strain rates along deep inherited faults, are required.

[34] Hereafter, we propose a scenario that mechanically explains the observed variations of plate strength, structural styles, and seismicity distribution using the stress/strain distribution (Figure 12). The Peikang basement high can be viewed as a strong and buoyant crustal asperity in the foreland which is hardly subducting beneath the Taiwan orogen. Owing to more frontal convergence on its southern flank, the expected level of compressional stresses arising from plate interaction is also higher. This is not dependent on the plate curvature. In this context, the presence of favorably oriented Paleogene normal faults south, in the Tainan basin, should contribute to a release of those stresses at higher strain rates. This contribution is consistent with the relative high level of seismicity south of the basement high (Figures 5a and 5b), indicating that the upper crust is closer to failure with regard to northward. A relative acceleration of strain rates in the upper crust implies a higher degree of crust/mantle decoupling. This explains why thick-skinned deformation is preferentially observed southward. Because of such a strain/stress distribution, the lower crust and lithospheric mantle become weaker by shifting the mechanically strong crust and mechanically strong lithosphere toward shallower depths (Figure 12). By contrast, northward, due to more oblique collision, strain rates are more homogeneously distributed in the crust (or higher in the lower crust), as it is illustrated by the pervasive distribution of the seismicity (Figures 5a and 5b); the lithosphere thus remains elastic and stronger. Crustal decouplings predicted at midcrust and at the base of the crust are less efficient; deformation at the belt front is thus transferred to shallower depth as suggested by thin-skinned deformation (Figure 12).

[35] Correlation between spatial variations of the flexural rigidity of the lithosphere and the nature and amount of foreland deformation has been also suggested for the Andes fold-and-thrust belt [*Watts et al.*, 1995]. Similarly, they observed that regions with low T_e correlate with thick-skinned deformation whereas regions with high T_e correlate with thin-skinned deformation. They proposed that a strong lithosphere is less easily deformed and the shortening can concentrate in a narrow zone at shallow depth. On the other hand, a weak lithosphere enables decoupling of the brittle crust and shortening. This study suggests how the local increase of plate coupling and inhomogeneities in a pre-fractured margin can affect the rigidity of a layered continental lithosphere and how its strength can be mechanically related to the structural style.

6. Conclusions

[36] The main conclusions can be summarized as follows:

[37] 1. Deformation in western Taiwan is characterized by a variable depth-frequency distribution of crustal earthquakes which is closely connected with along-strike variations of tectonic styles (thin or thick skinned) around the Peikang High, a major inherited feature of the Chinese margin.

[38] 2. The observed high surface heat flow and thermal age inherited from Paleogene rifting of the Chinese margin leads to a hot continental geotherm in the Eurasian continental lithosphere. Constraints on the brittle strength of the lithosphere from depth-frequency distribution of crustal earthquakes lead us to propose a Qz-diorite and granulite rheology for the upper and the lower crust. The Eurasian lithosphere appears to be more mafic and with higher strength than would be expected from more classical Qz-dominated rheology.

[39] 3. Flexural modeling reveals that the foreland basin can be explained by migration of thrust loads acting near the western deformation front. Using brittle-elastic-ductile plate rheology, the lithospheric flexure is modeled by T_e values of $\sim$15–20 km. These values can be attributed to different properties of the plate such as its thermal state, lithosphere rheology, and stress/strain distribution. Flexure modeling predicts that the crust is decoupled from the mantle, thus providing a mechanical explanation of how the basement-involved shortening is accommodated at depth.

[40] 4. Flexural modeling indicates a decrease of plate rigidity southward. An explanation is that the plate yields more easily southward because of plate curvature related to bending stresses and/or additional in-plane tectonic stresses at the plate boundary. First, the reduction of plate strength to the south of the Peikang High is not easily explained by the plate curvature. However, while bending stresses can explain extensional faulting in the outer foreland, they are unable to reproduce the distribution of seismic activity and compressive mechanisms closer to the deformation front. On the other hand, horizontal compressional stresses of 500–700 MPa are able to cause compressional brittle deformation in the upper crust throughout and are high enough to overprint flexurally controlled extension.

[41] 5. The Peikang basement high, which can be viewed as a strong and buoyant crustal asperity in the foreland, is hardly subducting beneath the Taiwan orogen. More frontal convergence on its southern flank and the presence of favorably oriented Paleogene normal faults south in the Tainan basin contribute to release stresses at higher strain rates in the upper crust. This is indicated by the relatively high level of seismicity south of the basement high. Because of this strain/stress distribution, the lower crust and lithospheric mantle appear weaker by shifting the mechanically strong crust and mechanically strong lithosphere toward shallower depths. By contrast, northward, due to more oblique collision, the lithosphere remains elastic and stronger.

[42] 6. This study suggests that when the Eurasian plate enters the Taiwan collision, tectonic inheritance of the continental margin can exert a strong control on the plate deformation by modifying its strength. One thus expects that in the past, inherited Paleogene basins and highs might have strongly influenced the growth and stability of the Taiwan mountain range by episodic accretion of weak/strong portions of the lithosphere.

[43] **Acknowledgments.** This work was supported by the Institut Français à Taipei-National Science Council of Taiwan cooperation framework and the French Ministry of Research. F. Mouthereau particularly thanks K.-M. Yang (CPC) and K.-F. Ma (NCU) for stimulating discussions. The authors are thankful to E. Burov for suggestions that greatly improve the manuscript. The authors also thank S.-K. Hsu for providing its compilation of Bouguer gravity data and E. Burov for providing his modeling code. The final form of the manuscript was greatly improved by the comments of C. Ebinger and two anonymous reviewers. We are also grateful to the associate editor Jerry Mitrovica for his insightful comments. Figures were prepared using the Generic Mapping Tool software [*Wessel and Smith*, 1998].

References

Barr, T. D., and F. A. Dahlen, Constraints on friction and stress in the Taiwan fold-and-thrust belt from heat flow and geochronology, *Geology*, *18*, 111–115, 1990.

Beaumont, C., P. Fullsack, and J. Hamilton, Styles of crustal deformation in compressional orogens caused by subduction of underlying lithosphere, *Tectonophysics*, *232*, 119–132, 1994.

Brace, W. F., and D. L. Kohlstedt, Limits on the lithospheric stress imposed by laboratory experiments, *J. Geophys. Res.*, *85*, 6248–6252, 1980.

Brudy, M., M. D. Zoback, K. Fuchs, F. Rummel, and J. Baumgartner, Estimate of the complete stress tensor to 8 km depth in the KTB scientific drill holes: Implications for crustal strength, *J. Geophys. Res.*, *102*, 18,453–18,475, 1996.

Burov, E. B., and M. Diament, The effective elastic thickness (T_e) of continental lithosphere: What does it really mean?, *J. Geophys. Res.*, *100*, 3905–3927, 1995.

Burov, E., L. Jolivet, L. Le Pourhiet, and A. Poliakov, A thermomechanical model of exhumation of high pressure (HP) and ultra-high pressure (UHP) metamorphic rocks in Alpine-type collision belts, *Tectonophysics*, *341*, 113–136, 2001.

Byerlee, J., Friction of rocks, *Pure Appl. Geophys.*, *116*, 615–626, 1978.

Chang, Y.-L., C.-I. Lee, C.-W. Lin, C.-H. Hsu, and E.-W. Mao, Inversion tectonics in the foothills of the Chiayi-Tainan area, southwestern Taiwan, *Petrol. Geol. Taiwan*, *15*, 199–217, 1996.

Chemenda, A. I., R.-K. Yang, J.-F. Stephan, E. A. Konstantinovskaya, and G. M. Ivanov, New results from physical modelling of arc-continent collision in Taiwan: Evolutionary model, *Tectonophysics*, *333*, 159–178, 2001.

Chen, H., Crustal uplift and subsidence in Taiwan: An account based upon retriangulation results, *Spec. Publ. Cent. Geol. Surv.*, *3*, 127–140, 1984.

Chen, W.-P., and P. Molnar, Focal depths of intracontinental earthquakes and their implications for the thermal and mechanical properties of the lithosphere, *J. Geophys. Res.*, *88*, 4183–4214, 1983.

Chiu, H. T., Basement rocks under the Neogene formation of west-central Taiwan, *Proc. Geol. Soc. China*, *16*, 51–58, 1973.

Cloetingh, S., and E. B. Burov, Thermomechanical structure of European continental lithosphere: Constraints from rheological profiles and EET estimates, *Geophys. J. Int.*, *124*, 695–723, 1996.

Dahlen, F. A., J. Suppe, and D. Davis, Mechanics of fold-and-thrust belts and accretionary wedges: Cohesive Coulomb theory, *J. Geophys. Res.*, *89*, 10,087–10,101, 1984.

Davis, D., J. Suppe, and F. A. Dahlen, Mechanics of fold-and-thrust belts and accretionary wedges, *J. Geophys. Res.*, *88*, 1153–1172, 1983.

Déverchère, J., F. Houdry, M. Diament, N. V. Solonenko, and A. V. Solonenko, Evidence for a seismogenic upper mantle and lower crust in the Baikal rift, *Geophys. Res. Lett.*, *18*, 1099–1102, 1993.

Déverchère, J., C. Petit, N. Gileva, N. Radziminovitch, V. Melnikova, and V. San'kov, Depth distribution of earthquakes in the Baikal rift system and its implications for the rheology of the lithosphere, *Geophys. J. Int.*, *146*, 1–26, 2001.

Ellwood, A., C.-Y. Wang, L. S. Teng, and H.-Y. Yen, Gravimetric examination of thin-skinned detachment vs basement-involved models for the Taiwan orogen, *J. Geol. Soc. China*, *39*, 209–221, 1996.

Goetze, C., The mechanics of creep in olivine, *Philos. Trans. R. Soc. London, Ser. B*, *288*, 99–119, 1978.

Hansen, F. D., and N. L. Carter, Creep of selected crustal rocks at 1000 MPa, *Eos Trans. AGU*, *63*, 437, 1982.

Harry, D. L., J. S. Oldow, and D. S. Sawyer, The growth of orogenic belts and the role of crustal heterogeneities in the decollement tectonics, *Geol. Soc. Am. Bull.*, *107*, 1411–1426, 1995.

Ho, C.-S., Foothills tectonics of Taiwan, *Bull. Geol. Surv. Taiwan*, *25*, 9–28, 1976.

Hsu, S.-K., C.-S. Liu, C.-T. Shyu, S.-Y. Liu, J.-C. Sibuet, S. Lallemand, C. Wang, and D. Reed, New gravity and magnetic anomaly maps in the Taiwan-Luzon region and their preliminary interpretation, *Terr. Atmos. Oceanic Stud.*, *9*, 509–532, 1998.

Hung, J.-H., D. V. Wiltschko, H.-C. Lin, J. B. Hickman, P. Fang, and Y. Bock, Structure and motion of the southwestern Taiwan fold and thrust belt, *Terr. Atmos. Oceanic Stud.*, *10*, 543–568, 1999.

Kao, H., and F. T. Wu, The 16 September earthquake (Mb = 6.5) in the Taiwan Strait and its tectonic implications, *Terr. Atmos. Oceanic Stud.*, *7*, 13–29, 1996.

Lacombe, O., Paleostress magnitudes associated with development of mountain belts: Insights from tectonic analyses of calcite twins in the Taiwan Foothills, *Tectonics*, *20*, 834–849, 2001.

Lacombe, O., and F. Mouthereau, Basement-involved shortening and deep detachment tectonics in forelands of orogens: Insights from recent collision belts (Taiwan, Western Alps, Pyrenees), *Tectonics*, *21*(4), 1030, doi:10.1029/2001TC901018, 2002.

Lallemand, S., Y. Font, H. Bijwaard, and H. Kao, New insights on 3-D plates interaction near Taiwan from tomography and tectonic implications, *Tectonophysics*, *335*, 229–253, 2001.

Lee, T.-Y., and L. A. Lawver, Cenozoic plate reconstruction of Southeast Asia, *Tectonophysics*, *251*, 85–138, 1995.

Lin, A. T., and A. B. Watts, Origin of the West Taiwan basin by orogenic loading and flexure of the rifted continental margin, *J. Geophys. Res.*, *107*(B9), 2185, doi:10.1029/2001JB000669, 2002.

Liu, C.-S., S.-Y. Liu, B.-Y. Kuo, N. Lundberg, and D. L. Reed, Characteristics of the gravity and magnetic anomalies off southern Taiwan, *Acta Geol. Taiwan*, *33*, 121–130, 1992.

Ma, K.-F., and D.-R. Song, Pn velocity and Moho depth in Taiwan, *J. Geol. Soc. China*, *40*, 167–184, 1997.

Maggi, A., J. A. Jackson, D. McKenzie, and K. Priestley, Earthquake focal depths, effective elastic thickness, and the strength of the continental lithosphere, *Geology*, *28*, 495–498, 2000.

Malavieille, J., S. Lallemand, S. Dominguez, A. Deschamps, C.-Y. Lu, C.-S. Liu, P. Schnürle, and A. S. Crew, Arc-continent collision in Taiwan: New marine observations and tectonic evolution, in *Geology and Geophysics of an Arc-Continent Collision, Taiwan, Republic of China*, edited by T. B. Byrne and C.-S. Liu, pp. 187–211, Geol. Soc. of Am., Boulder, Colo., 2002.

Mouthereau, F., O. Lacombe, B. Deffontaines, J. Angelier, and S. Brusset, Deformation history of the southwestern Taiwan foreland thrust belt: Insights from tectono-sedimentary analyses and balanced cross-sections, *Tectonophysics*, *333*, 293–322, 2001.

Mouthereau, F., B. Deffontaines, O. Lacombe, and J. Angelier, Variations along the strike of the Taiwan thrust belt: Basement control on structural style, wedge geometry and kinematics, in *Geology and Geophysics of an Arc-Continent Collision, Taiwan, Republic of China*, edited by T. B. Byrne and C.-S. Liu, pp. 35–58, Geol. Soc. of Am., Boulder, Colo., 2002.

Rau, R.-J., and F. T. Wu, Tomographic imaging of lithospheric structures under Taiwan, *Earth Planet. Sci. Lett.*, *133*, 517–532, 1995.

Sandwell, D. T., and W. H. F. Smith, Marine gravity anomaly from Geosat and ERS 1 satellite altimetry, *J. Geophys. Res.*, *102*, 10,039–10,054, 1997.

Seno, T., S. Stein, and A. E. Gripp, A model for the motion of the Philippine Sea plate consistent with NUVEL-1 and geological data, *J. Geophys. Res.*, *98*, 17,941–17,948, 1993.

Sibson, R. H., Frictional constraints on thrust, wrench and normal faults, *Nature*, *249*, 542–544, 1974.

Suppe, J., A retrodeformable cross section of northern Taiwan, *Proc. Geol. Soc. China*, *23*, 46–55, 1980.

Suppe, J., Mechanics of mountain building and metamorphism in Taiwan, *Geol. Soc. China Mem.*, *4*, 67–89, 1981.

Suppe, J., Kinematics of arc-continent collision, flipping of subduction, and back-arc spreading near Taiwan, *Geol. Soc. China Mem.*, *4*, 67–90, 1984.

Suppe, J., and J. H. Wittke, Abnormal pore-fluid pressures in relation to stratigraphy and structure in the active fold-and-thrust belt of northwestern Taiwan, *Petrol. Geol. Taiwan*, *14*, 11–24, 1977.

Teng, L.-S., C.-T. Lee, Y.-B. Tsai, and L.-Y. Hsiao, Slab breakoff as a mechanism for flipping of subduction polarity in Taiwan, *Geology*, *28*, 155–158, 2000.

Watts, A. B., and E. B. Burov, Lithospheric strength and its relationship to the elastic and seismogenic layer thickness, *Earth Planet. Sci. Lett.*, *213*, 113–131, 2003.

Watts, A. B., S. H. Lamb, J. D. Fairhead, and J. F. Dewey, Lithospheric flexure and bending of the central Andes, *Earth Planet. Sci. Lett.*, *134*, 9–21, 1995.

Wessel, P., and W. H. F. Smith, New version of the generic mapping tools released, *Eos Trans. AGU*, *79*, 579, 1998.

Wilks, K. R., and N. L. Carter, Rheology of some continental lower crust, *Tectonophysics*, *182*, 57–77, 1990.

Willett, S. D., Orogeny and orography: The effects of erosion on the structure of mountain belts, *J. Geophys. Res.*, *104*, 28,957–28,981, 1999.

Wu, F. T., R.-J. Rau, and D. Salzberg, Taiwan orogeny: Thin-skinned or lithospheric collision, *Tectonophysics*, *274*, 191–220, 1997.

Yang, K.-M., S.-T. Huang, J.-C. Wu, M. Lee, H.-H. Ting, and W.-W. Mei, The characteristics of subsurface structure and evolution of the Tachienshan-Chukou thrust system, in *Annual Meeting of the Geological Society of China*, pp. 82–84, Geol. Soc. of Taiwan, Chiayi, Taiwan, 2001.

Yen, H.-Y., Y.-H. Yeh, C.-H. Lin, G.-K. Yu, and Y.-B. Tsai, Free-air gravity map of Taiwan and its application, *Terr. Atmos. Oceanic Stud.*, *1*, 143–156, 1990.

Yen, H.-Y., Y.-H. Yeh, and F. T. Wu, Two-dimensional crustal structures of Taiwan from gravity data, *Tectonics*, *17*, 104–111, 1998.

Yu, H.-S., and Y.-W. Chou, Characteristics and development of the flexural forebulge and basal unconformity of western Taiwan foreland basin, *Tectonophysics*, *333*, 277–291, 2001.

Yu, S.-B., H.-Y. Chen, and L.-C. Kuo, Velocity field of GPS stations in the Taiwan area, *Tectonophysics*, *274*, 41–59, 1997.

Ziegler, P. A., J.-D. van Wees, and S. Cloetingh, Mechanical controls on collision-related compressional intraplate deformation, *Tectonophysics*, *300*, 103–129, 1998.

Zoback, M. D., and J. H. Healy, In situ stress measurements to 3.5 km depth in the Cajon Pass scientific research borehole: Implications for mechanics of crustal faulting, *J. Geophys. Res.*, *97*, 5039–5058, 1992.

F. Mouthereau and C. Petit, Laboratoire de Tectonique, UMR7072, UPMC, Case 129 T 26 E1, 4 Place Jussieu, F-75252 Paris Cedex 05, France. (frederic.mouthereau@lgs.jussieu.fr)